AD-A069 595 VARIAN ASSOCIATES BEVERLY MASS F/G 9/5
HIGH POWER MICROWAVE MULTIPACTOR SWITCH, DRIVER AND FEASIBILITY--ETC(U)
NOV 76 N00173-76-C-0294
UNCLASSIFIED NL

END
DATE FILMED
7-79
DDC

(1)

LEVEL II

p.3 is poor 1

AD A069595

Varian/Beverly,
VDU-1073. Progress Report.
HIGH POWER MICROWAVE MULTIPACTOR SWITCH, DRIVER AND FEASIBILITY STUDY.
27 pgs., November 11, 1976

UNCLASSIFIED

NRL 542235

Copy # (Rec'd) Date
1--5-31-79

Copy # (Dest) Date

N00173-76-C-0294
(NRL Contract)
5250,2
Reus

DDC FILE COPY

DDC
RECEIVED
JUN 8 1979
E

DISTRIBUTION STATEMENT A
Approved for public release;
Distribution Unlimited

79 06 04 041

(9) PROGRESS REPORT, Jul – 1 Oct 76,

(6) HIGH POWER MICROWAVE MULTIPACTOR SWITCH, DRIVER AND FEASIBILITY STUDY

VDU-1073,

Contract No.

(15) N00173-76-C-0294

NAVAL RESEARCH LABORATORY

Washington, D. C. 20930

APPROVED FOR PUBLIC RELEASE
DISTRIBUTION UNLIMITED

Accession For	
NTIS GRA&I	X
DDC TAB	
Unannounced	
Justification	
By	
Distribution/	
Availability Codes	
Dist.	Avail and/or special
A	

Prepared by

VARIAN/~~BEVERLY~~ Associates

Eight Salem Road

Beverly, Massachusetts 01915

(11) 11 Nov~~ember~~ 1976

(12) 30 p.

364 070

TABLE OF CONTENTS

I. INTRODUCTION

This is a progress report, covering the period from July to 1 October 1976, on the development of the VDU-1073, a single pole, single throw multipactor switch, being developed under Contract No. N00173-76-C-0294. The desired specifications of the switch are included in Figure I-1.

The program also includes a feasibility study for a 50 KW, 50 per cent duty cycle multipactor switch which will operate from 8.2 to 12.4 GHz or one which will operate from 12.4 to 18 GHz. Program status is indicated in Figure I-2.

The devices being built are designed with flexibility in mind, so that circuit components can be interchanged to achieve desired power levels, bandwidths, operating frequencies, etc. Initially under consideration are ridged waveguide and comb line structures. The way in which these circuits should work in a multipactor switch is described in the body of the report.

Assembly has begun on Engineering Development Model No. 1 (EDM 1), which is shown in Figure I-3. The device is designed around ridged waveguide with a 2.4:1 bandwidth in J-band. The gap between the ridge is tapered in order to provide multipactor at a lower power level near the output of the device. This should enable the switch to operate over a wider power range.

EDM 1 is designed so that all elements, including vacuum seal windows, the modulating electrode, the circuit, the oxygen source, and the Vac-Ion pump can be interchanged or replaced with other elements as the development of the device proceeds. The top cover is heliarc welded and can be easily removed. For example, a comb line structure, as described in the body of this report, will be used in future models. This type of structure should allow the multipactor switch to operate at a lower power level than with the ridged waveguide. These changes can be made after a hot test (high power) on the tube.

A filter section is designed into the modulating electrode to minimize propogation of undesired modes through the switch.

FIGURE I-1

Type	Single pole, single throw
Center Frequency	15 GHz
Bandwidth	10 per cent (15 per cent design goal)
VSWR	1.5:1 maximum both states
Switching Time	3 nanoseconds maximum
Power Level	4.75 watts to 3 KW peak
Duty Cycle	10 per cent
Isolation	28 dB minimum at 3 KW
Insertion Loss	1 db in transmit state

varian

FIGURE 1 PROGRAM PLAN -VDU1073

MASTER PLAN

PROGRAM: "J" BAND (WR-2) MULTIPACTOR SWITCH

PROGRAM SCHEDULE - MONTHS ARO, (JULY 1976)

CONTRACT:

TASK DESCRIPTION	1	2	3	4	5	6	7	8	9	10
1. Basic Design										
2. Order, Fabricate & Evaluate Cold Tester										
3. Check Out Test Set										
4. Order & Fabricate Engineering Development MDL No.1 EDM 1										
5. Hot Test EDM 1										
6. Order & Fabricate EDM 2										
7. Test EDM 2										
8. Modify EDM-1-1										
9. Test EDM-1-1										
10. Order & Fabricate EDM-3										
11. Test EDM-3										
12. Modify EDM-2-1										
13. Test EDM-2-1										
14. Quarterly Reports (Including Feasibility)										
15. Final Report										
16. Feasibility Report (Final)										

FIGURE I-2

PLANCODE:

△ Forecast Start Date
▽ Previous Start Date
○ Open-To Be Scheduled
▲ Forecast Finish Date
▼ Previous Finish Date
◆ Completed

Form No. 55011 Sept. 1969

Plan No. 1
Date Released [illegible]
Date Updated 11/4/75 Page 1 Of 1

ENGINEERING DEVELOPMENT

MODEL NUMBER 1

VDU-1073

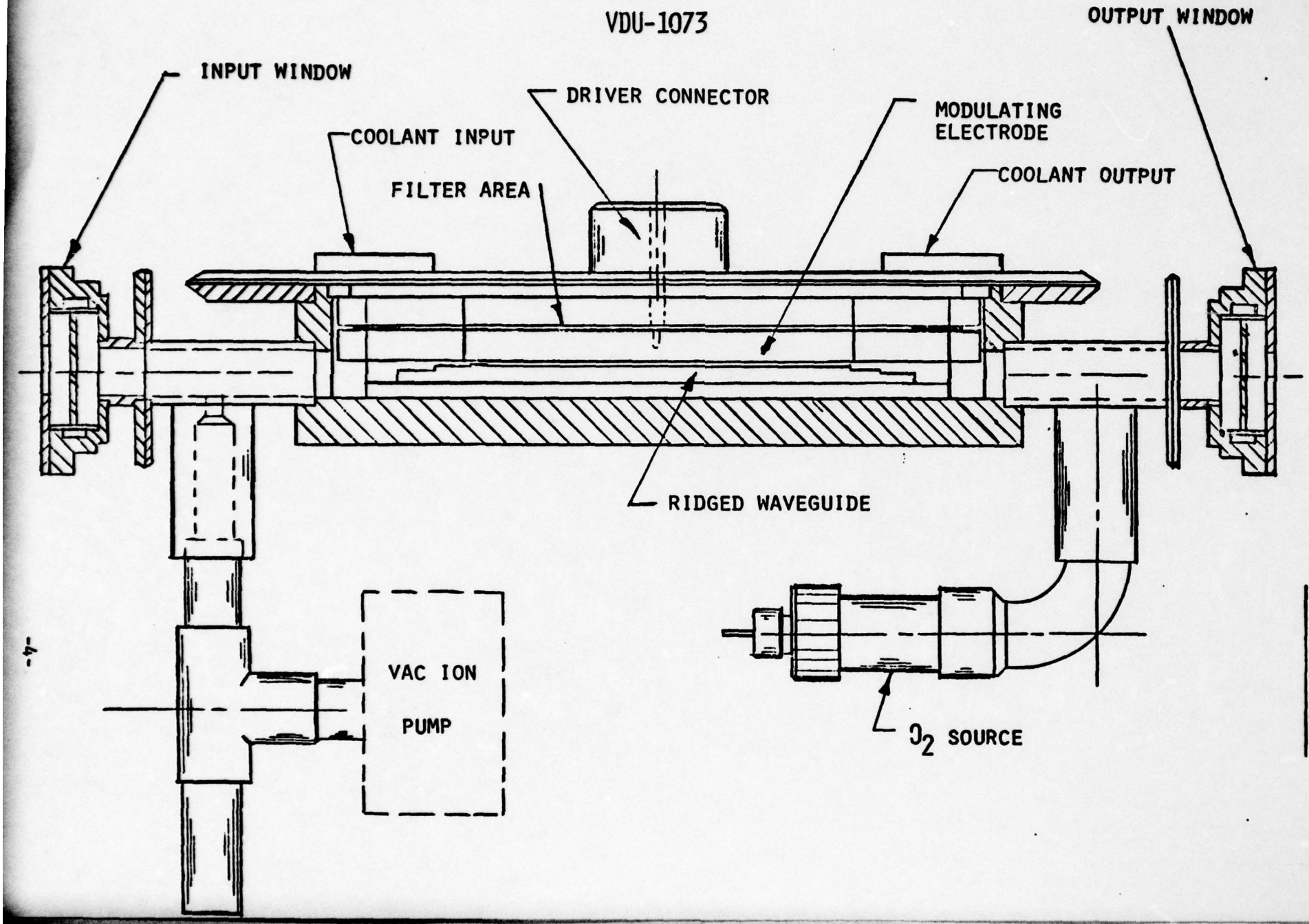

FIGURE I-3

Information gained by experiments with various types of circuit elements will be used in the feasibility study to point the way towards the design of a multipactor switch with greater bandwidth and higher power capability.

The remainder of this report is divided into five sections.

Section II describes the multipactor process and how it can be exploited to produce a multipactor switch.

Section III describes the design of Engineering Development Model No. 1.

Section IV describes the analysis of the comb line structure to be used in future experimental models. Expected performance is presented.

Section V describes tests made on small sections of circuit structures under consideration. It is shown how RF parameters, important for proper multipactor operation, can be measured with these sections before they are incorporated into the actual switch.

Section VI is a summary of the report and of progress so far.

II. THE THEORY OF THE MULTIPACTOR SWITCH

A. Multipactor

The multipactor process is a resonance phenomenon which manifests itself at high power levels. To understand its operation, consider the geometry of Figure II-1.

The space between the metal plates is evacuated, and there is an electron in the space. An electric field perpendicular to the plates will cause the electron to accelerate towards one of the plates. The plates are coated with secondary emitting material which will yield an increased number of electrons for an average striking electron. The ratio of electrons emitted to electrons striking is called the secondary emission coefficient (δ). This coefficient is a function of the energy with which electrons strike the material.

Now consider what happens when the driving electric field is due to RF power. If the electron impact energy is such that the secondary emission coefficient is greater than one, the alternating electric field will cause electrons emitted at one plate to strike the opposite plate, where if the striking energy is again proper, still more electrons will be generated. If there were originally N electrons in the gap, after m RF half cycles, there will be N^m electrons. Since the RF field must give up energy to create this electron cloud, a multipactor device is seen to act as a limiter with a turn-on time of only several cycles. If 10^{10} electrons represents the saturated discharge within the gap, and a secondary emission ratio of 5 is assumed, then space charge limited operated will result in approximately 7-1/2 RF cycles, or at 15 GHz, in 0.5 nanoseconds. The process also stops after one-half RF cycle. The result is a limiter with a very fast turn-on and turn-off time.

FIGURE II-1

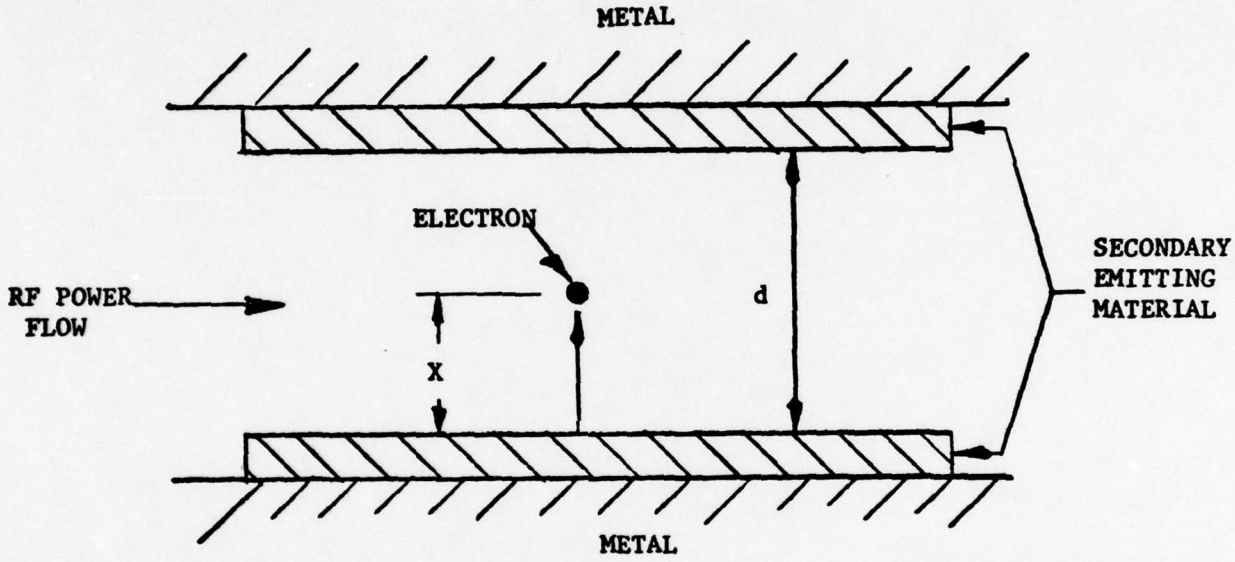

MULTIPACTOR GEOMETRY

For the initial design, a simple model has been used to predict the conditions necessary to achieve multipactor. Referring to Figure II-1, and using the relations

$$\bar{F} = m \ddot{\bar{x}}$$

and

$$\bar{F} = -e \bar{E}$$

it is found that for the electron's acceleration, $\ddot{x}$

$$\ddot{x} = -\eta \frac{V}{d}$$

where

F = force on the electron

m = mass of the electron

e = electron charge

η = e/m

E = electric field in the gap

V = voltage between the plates

d = distance between the plates.

It is assumed that $\bar{E}$ is uniform in the gap.

Assuming that $V = V_0 \sin \omega t$,

$$X = \frac{-\eta}{2} \frac{V_0}{d} \left[\sin \phi_0 - \sin \phi + (\phi - \phi_0) \cos \phi_0\right]$$

where

$\phi = \omega t$

$\phi_0 = \omega t_0$ is the phase angle at the time the electron starts across the gap.

Now, at resonance, when $x = d$, $\phi = M\pi$. Assuming $\phi_0 = 0$, and denoting the peak RF voltage necessary for resonance as V_r, it is found that

$$V_r = \frac{d^2\omega^2}{\eta M\pi} \qquad \text{II-1}$$

To find the striking energy, V_i of the electron, expressed in electron volts, the relationship

$$e\,V_i = \frac{1}{2}\,m\,\dot{x}^2 \Big|_{x = d,\ \phi = M\pi}$$

is used to find

$$V_i = \frac{2}{M\pi}\,V_r \qquad \text{II-2}$$

M must be an odd number, and M/2 is called the order of the multipactor mode.

Now, Figure II-2 shows the relationship between secondary emission coefficient (δ) and striking energy (V_i) for any secondary emission material. V_i is about 20 eV and V_2 about 2000 eV for materials under consideration.

Equation II-2 fixes the limits on V_r for multipactor to occur and equation II-1 fixes d for a given V_R. Equation II-1 was derived assuming $\phi_0 = 0$. For different V_r for a fixed gap d, ϕ_0 will vary. Multipactor should still occur for a range of ϕ_0.

Defining an impedance, Z_0, by the relationship

$$Z_0 = \frac{V_Z^2}{2P} \qquad \text{II-3}$$

where P is the power flowing through the multipactor structure which will give rise to a peak RF voltage V_Z in the multipactor gap.

Equations II-1, II-2, and II-3 have been used in the design of the first Engineering Development Model to predict the power levels for multipactor to occur. The effects of interaction

FIGURE II-2

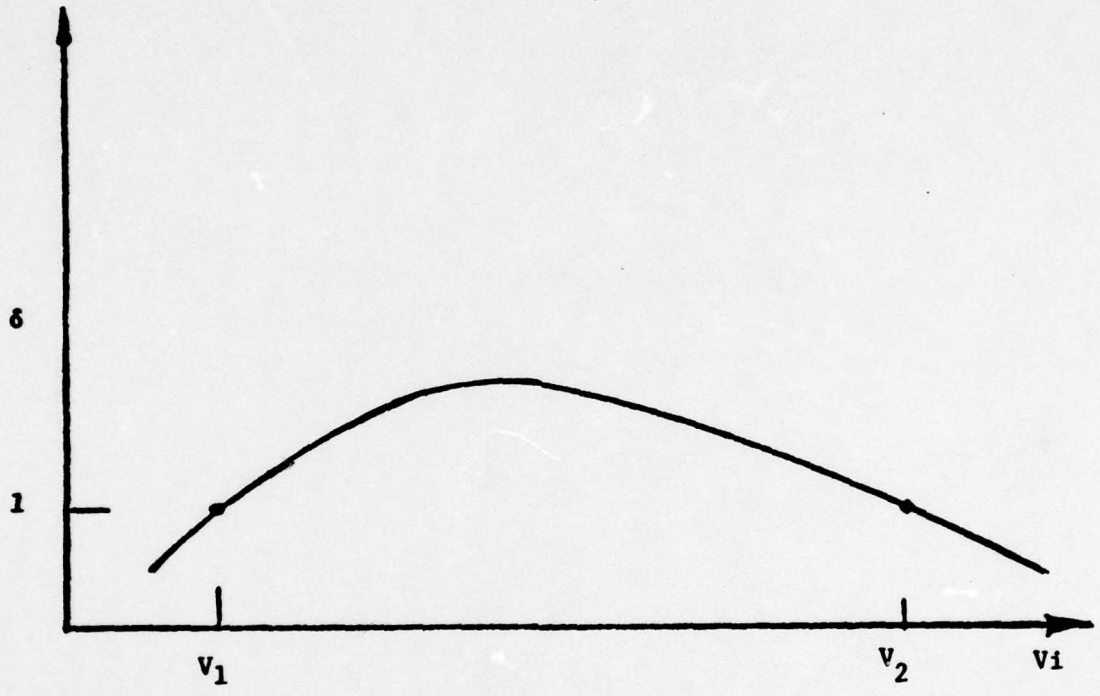

RELATIONSHIP BETWEEN IMPACT ENERGY (Vi) AND SECONDARY EMISSSION COEFFICIENT (δ)

between electrons in the cloud and of non-zero starting phase for the electrons have been ignored. Equations II-1, II-2, and II-3 should only be considered as giving rough estimates so an initial experimental device can be designed. The details of this design are given in the section on the design of Engineering Development Model Number One.

A more complete analysis of the multipactor process has been done by Forrer and Millazzo[1]. It is planned to carry out a similar analysis for the multipactor switch.

B. A Multipactor Switch

If an external voltage is applied between the plates, as shown in Figure II-3, a multipactor switch results. V_{mod} is always greater than zero. When V_{mod} is near zero, the multipactor process can occur at proper RF power levels. When V_{mod} is high enough, electrons will strike one plate with a V_i too large and the other plate with a V_i too small for multipactor to occur. As a result, the multipactor process will stop and the RF energy will proceed through unattenuated. It is seen that what we have is absorbtive modulation of the RF energy.

A pulse or square wave generator could be used in place of the sine wave generator shown in Figure II-3.

FIGURE II-3

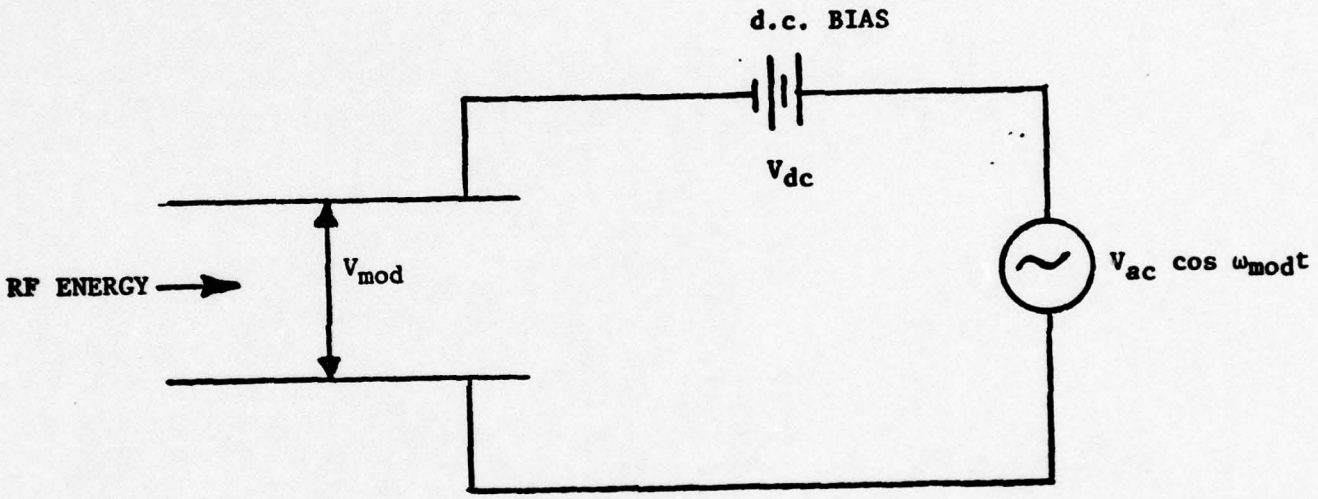

$$V_{mod} = V_{dc} + V_{ac} \cos \omega_{mod} t$$

MULTIPACTOR SWITCH

III. DESIGN OF ENGINEERING DEVELOPMENT MODEL NUMBER ONE

The design of the first Engineering Development Model of the multipactor switch was completed in September and all parts have been ordered. It is expected that tests will begin in December.

This section describes the design of the device. An overview of it is given in Figure I-3. Multipacting should occur in the gap of the ridged waveguide.

The modulating electrode is insulated from the body so that the modulating signal can be applied to it. Cooling fluid will flow through the modulating electrode. Input and output windows provide a vacuum seal. The Vac-Ion pump maintains low pressure in the device. The secondary emitting material is beryllium oxide. The modulating electrode and the top of the ridged guide will have beryllium or beryllium copper surfaces. The O_2 source will keep a layer of beryllium oxide on these surfaces. The O_2 source is located near the output and the Vac-Ion pump near the input to provide optimum O_2 availability for surface conditioning.

A. Expected Levels of Multipacting

The ridged waveguide tapers from a calculated impedance, Z_0, of 81 ohms, and a gap, d, of .037 cm at the input side to a Z_0 of 86 ohms and d of .013 cm at the output end. For beryllium oxide, V_i is between 20 and 2000 volts for secondary emission coefficient values of one or greater. Using equation II-2, we find V_r to be between about 32M and 3140M volts, where M/2 is the order of the multipacting mode.

For the gap of .037 cm, operation in the 3/2 mode will yield a V_r of 774 volts, a V_i of 164 volts, and a power level at resonance of 2400 watts. For the .013 cm gap, operation in the 1/2 mode results in a V_r of 300 volts, a V_i of 191 volts, and a power level at resonance of 300 watts. For operation of the .013 cm gap in the 3/2 mode, values of V_r of 63 volts, V_i of 13 volts (perhaps too low), and a power level of 23 watts are found.

B. Expected Bandwidth

The ridged waveguide is broad band and should have a usable range of 13 GHz to over 20 GHz. The four section impedance matching transformers on each end theoretically will provide a match VSWR of better than 1.01:1 over a 15 per cent bandwidth. A window has been tested to have an insertion loss of less than 0.2 dB over a 10 per cent bandwidth centered at 15 GHz. A sharp resonance resulting in an insertion loss of about 3 dB was noted at a frequency near, but below, the desired band of operation. Windows with several slightly different dimensions are being made in order to find the best window size for optimum bandwidth.

The windows are heliarced in place so that improvements in design can be incorporated as the design warrants.

IV. ANALYSIS OF COMB LINE STRUCTURES

In order for the multipactor phenomena to occur at power levels of a few watts, impedances of about 500 to 600 ohms are needed. This is not practical for a ridged waveguide structure so an analysis of a comb line structure was begun.

A section of a dual comb line is illustrated in Figure IV-1. An analysis has been carried out of this structure to find the impedance, Z_0, defined by equation II-3, where V_Z is now defined as the voltage across the multipactor gap. This analysis indicates that impedances from 100 to 600 ohms or greater should be achievable with this structure.

This analysis indicates that operation down to several watts can be achieved with the comb line.

FIGURE IV-1

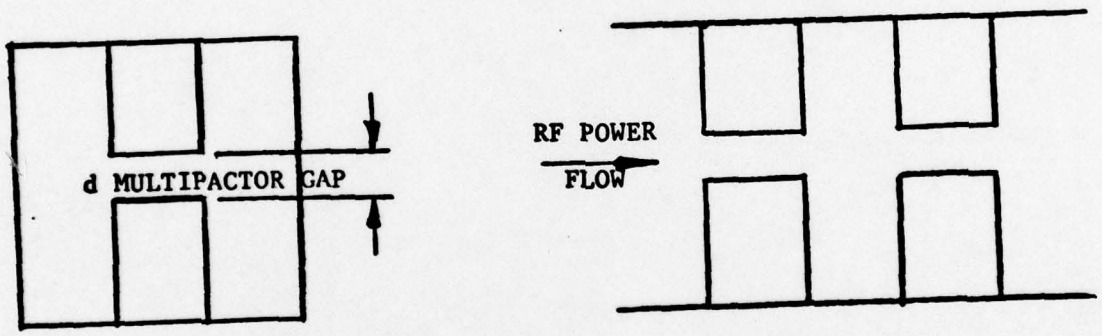

COMB LINE

V. COLD TESTER MEASUREMENTS

One inch sections of ridged waveguide were made. These duplicate the geometry of the ridged guide to be used in the first Engineering Development Model (described in the previous section), including a modulating electrode insulated from the body. One has a ridge gap of .037 cm and a ridge width of .127 cm. The other has a gap of .013 cm and a width of .026 cm. The calculated impedance at 15 GHz and cutoff frequency are given in Table 1.

Table 1 -- Calculated Values for Ridged Guide

Unit	d	W	f_c	Z_0 (15 GHz)
1	.037 cm	.127 cm	10.5 GHz	81 ohms
2	.013 cm	.026 cm	11.2 GHz	86 ohms

This section describes experiments performed in order to measure the impedance and guide wavelength of these cold testers. A cold tester version of a comb line structure is being produced, and similar tests will be performed on it. In this section we show how perturbation theory can be used to calculate the impedance of both the ridged guide and cold tester structure.

In order to measure guide wavelength, the input and output of the one inch cold tester sections were fed directly from rectangular waveguide with no impedance matching. This formed a resonant cavity of a length, ℓ, of one inch. At frequencies where the guide wavelength, λg, is such that $\frac{n\lambda g}{2} = 1$, transmission through the cavity was observed. In this way, λg is known at these frequencies, and a λg vs. f, which conveys the same information as an ω-β diagram, may be produced. The knowledge of how many half wavelengths a particular resonance corresponds to is based in part on theoretical calculations of cutoff frequency.

The measurment of impedance is based on perturbation theory. If a small amount of material of relative dielectric constant ε_r is placed in a resonant cavity, the frequency of resonance will shift by an amount of Δ_f, where[2]

$$\frac{\Delta_f}{f_o} \approx - \frac{\int_{\Delta V} \Delta\varepsilon \; E_{int} \cdot E_o^* \, dv}{2\int_V \varepsilon_o |E_o|^2 \, dv} \qquad \text{V-1}$$

Where

f_o = frequency of resonance with no dielectric in the cavity

ΔV = volume occupied by the dielectric perturber

V = volume of the cavity

E_{int} = electric field inside the perturber

E_o = electric field in the cavity with no dielectric perturber

ε_o = permittivity of free space

$$\Delta\varepsilon = \varepsilon_r \, \varepsilon_o - \varepsilon_o$$

The resonant frequency must always decrease when the perturber is added.

First impedance must be related to quantities in equation V-1.

At resonance

$$2 \int_V \varepsilon_o |E_o|^2 \, dv = 4 \, W_s$$

where W_s is the energy in the standing wave in the cavity. The energy in an equivalent travelling wave W_T will be twice that in a standing wave.

The power, P, flowing through the structure is given by

$$P = \frac{W_T}{\ell} \; V_g = \frac{W_T}{\ell} \; c \; \frac{\lambda_o}{\lambda_g}$$

FIGURE V-1

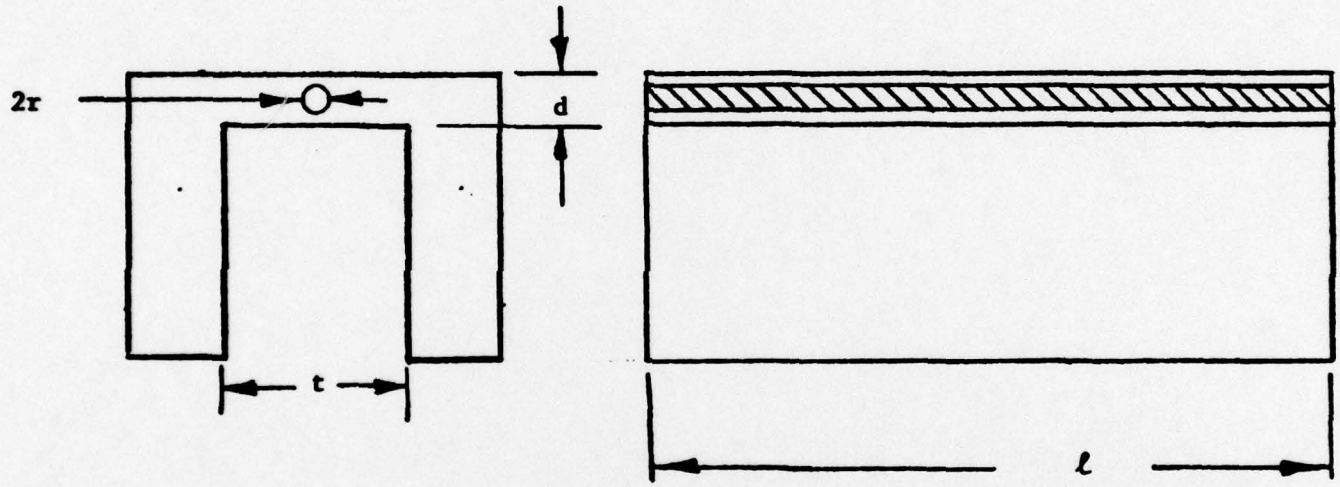

RIDGED GUIDE PERTURBATION

V_g = group velocity

ℓ = length of the cavity

c = velocity of free space

λ_o = free space wavelength

λ_g = waveguide wavelength.

Geometries such as that shown in Figure II-1 were considered where the electric field is uniform in the gap. Power can then be expressed in terms of impedance as

$$P = \frac{|E_g|^2 \, d^2}{2 \, Z_o}$$

where E_g is the electric field in the gap.

Continuing

$$2 \int_V \varepsilon_o |E_o|^2 \, dv = \frac{|E_g|^2 \, d^2 \, \ell \, \lambda_g}{Z_o \, c \, \lambda_o} \qquad \text{V-2}$$

Consider first perturbation measurements of the ridged guide, shown in Figure V-1. A strand of dielectric is threaded over the ridge. The relative dielectric constant of the strand is ε_r and its radius is r. If the electric field outside the strand is E_g, the field inside the strand, E_{int}, will be given by

$$E_{int} \approx \frac{2}{1 + \varepsilon_r} \, E_g \qquad \text{V-3}$$

Using equations V-2 and V-3 in V-1, and integrating in the cylindrical volume of the strand, we get the result

$$\left| \frac{\Delta f}{f_o} \right| = Z_o \, c \left(\frac{\lambda_g}{\lambda_o} \right) \frac{\varepsilon_o \, (\varepsilon_r - 1) \, 2 \pi \, r^2}{d^2 \, (1 + \varepsilon_r)}$$

The situation for the comb line is shown in Figure V-2. It would be desirable to have perturbation material only in the multipactor gaps, but this is not practical.

The dielectric is actually strung over the entire length, but since the electric field is strongest in the gaps, we consider the perturber to be only in the gaps.

FIGURE V-2

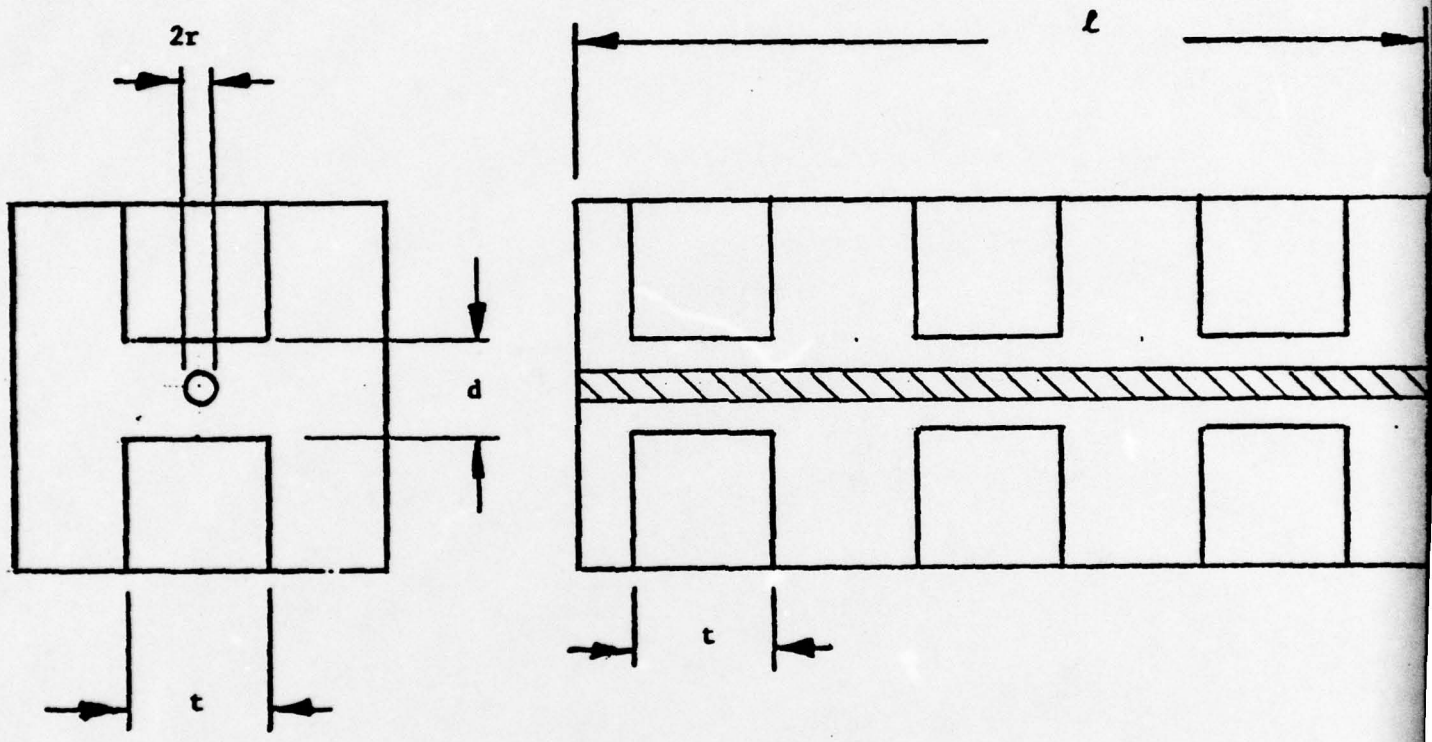

COMB LINE PERTURBATION

For the comb line

$$\left|\frac{\Delta f}{f_o}\right| = z_o\, c \left(\frac{\lambda_g}{\lambda_o}\right) \frac{Nt}{\ell} \quad \frac{\varepsilon_o (\varepsilon_r - 1)\, 2\pi r^2}{d^2 (1 + \varepsilon_r)}$$

where

N = number of gaps.

The experiment was performed on ridged units, numbers one and two, of Table 1 using nylon thread ($\varepsilon_r = 3$). Table 2 shows the results for unit number one.

Table 2 -- Resonant Frequencies (GHz)
for Unit No. 1

Thread Dia.	Unperturbed Freqs	Perturbed Freqs
.038 mm	13.308, 14.787	13.319, 14.770
.035 mm	13.327, 14.796	13.316, 14.778

The 13.3 GHz resonance with .038 mm thread indicated an increase in frequency when perturbed, which is not possible. The 14.7 GHz resonance with .038 mm thread, and 13.3 GHz and 14.796 GHz resonances with .035 mm thread indicated impedances of 50, 59, and 58 ohms respectively.

Considering that the experiment was relatively crude, the agreement of these values with the theoretical impedance of 81 ohms is remarkably good. A plot of λ_g vs. f for unit number one, using a resonance observed at K-band for the unperturbed unit is shown in Figure V-3. One resonance was observed in X-band so the 13.3 GHz resonance was plotted at $\lambda_g = 2.54$ cm.

For unit number two, only one good set of measurements was obtained. The results are shown in Table 3.

GUIDE WAVELENGTH OF UNIT NUMBER 1

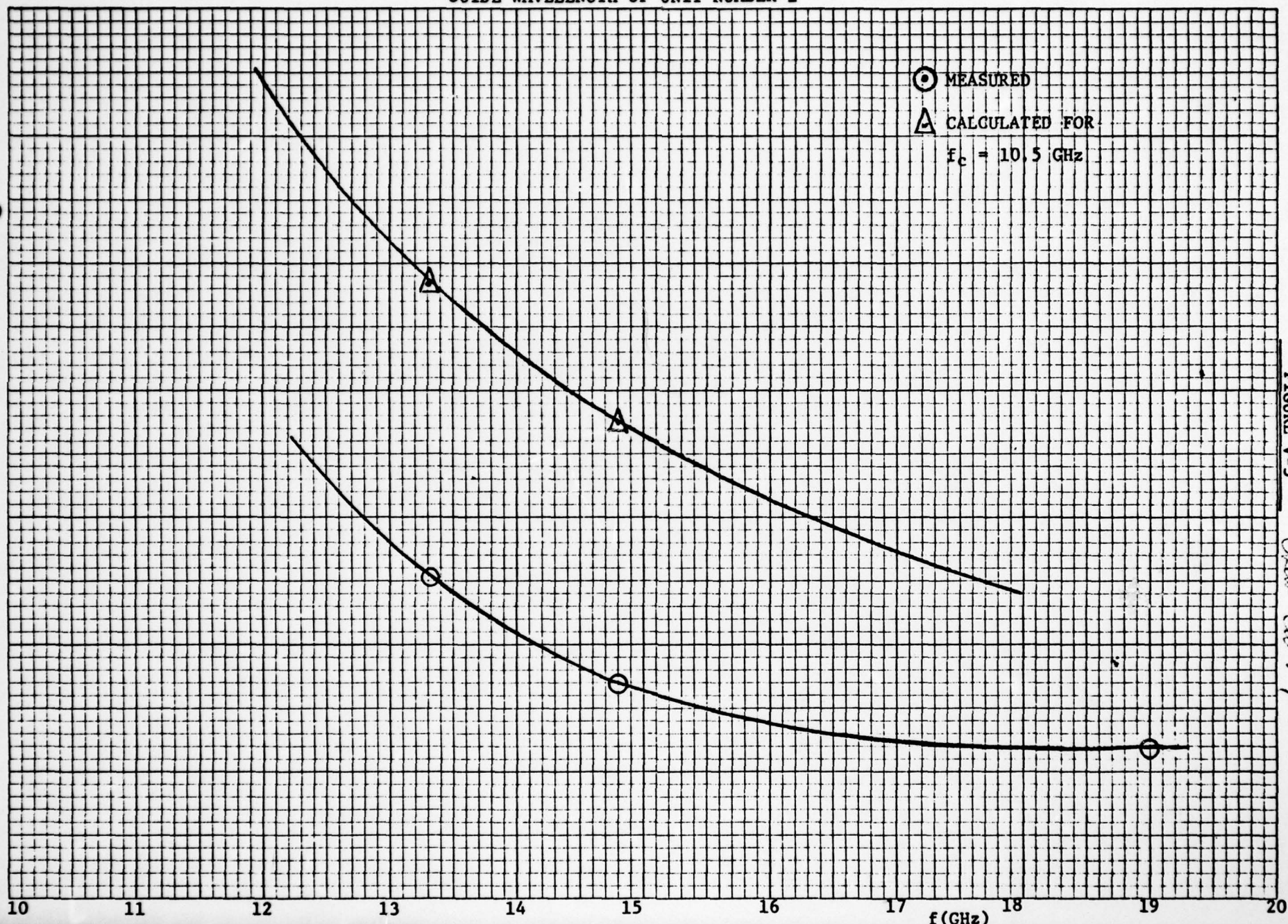

FIGURE V-3

Table 3 -- Resonant Frequencies (GHz)
for Unit No. 2

Thread Dia.	Unperturbed Freqs	Perturbed Freqs
.035 mm	13.265, 14.437	13.108, 14.220

Two two resonances at 13.3 and 14.4 GHz indicate impedances of 86 and 79 ohms respectively. Again, the results seem reasonable. A λ_g vs. f curve for unit number 2 is shown in Figure V-4. Again, one resonance was observed in X-band.

It seems that the perturbation technique described in this section should prove to be a useful technique for determining the impedance of structures under consideration for the multipactor switch.

Looking at the λ_g vs. f diagrams of both ridged guides, it is seen that λ_g is shorter than would be predicted from the calculated cutoff frequencies. This is indicative of fast wave propogation through an undesired RF path around the modulating electrode. However, the measured impedances are close to what they should be, indicating that close to the desired amount of power is being concentrated in the multipacting gap. Any significant coupling of energy through an undesired path should cause an appreciable decrease in the measured impedance.

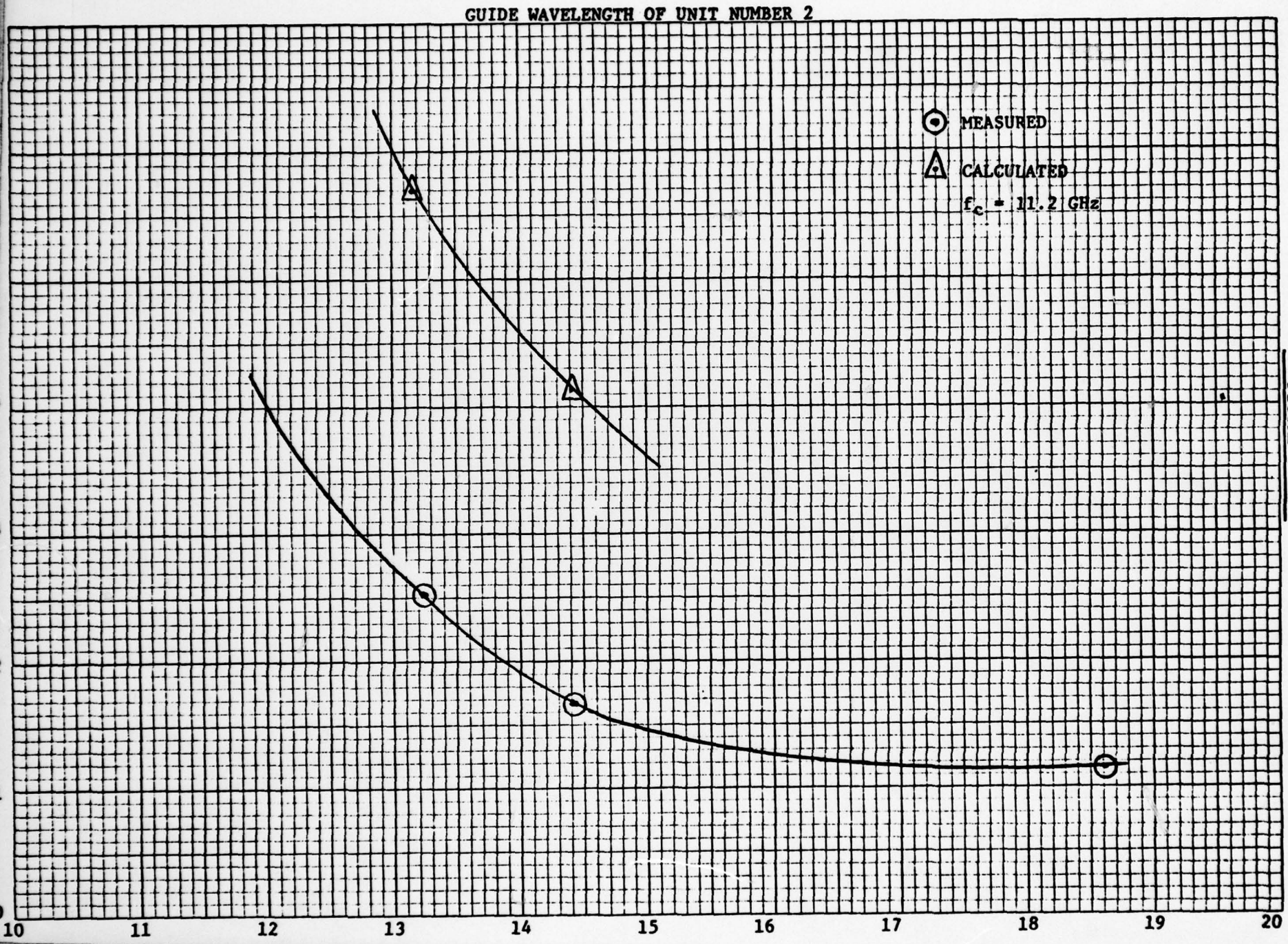

FIGURE V-4

VI. SUMMARY

Design and development are continuing on a multipactor switch which should meet the requirements of Figure I-1. Assembly has begun on Engineering Development Model One as described in Section III. In its initial configuration, EDM 1 is designed to meet all the requirements of Figure I-1 except power level, which should be from about 35 watts to 3 kW peak. The components of the unit are easily replaced with others of different design, such as the comb line described in Section IV. By exploiting this interchangeability feature, Varian plans to reach the goals of Figure I-1 and to point the way towards the design of multipactor switches with higher power capability and broader bandwidth. Section 5 shows how, by using small sections of circuit structures under consideration, RF properties of these structures important for proper multipactor operation can be measured before incorporation into the actual switch. The methods described in this section are currently being used to analyze the comb line structure.

REFERENCES

1. Forrer, M. P., and Milazzo, C., High Power Microwave Duplexing and Switching Using Multipactor Discharges in High Vacuum; General Electric Power Tube Division Report No. R61ELM212, August, 1961.

2. Harrington, R. F., Time Harmonic Electromagnetic Fields; McGraw Hill, 1961, Chapter 7.